

A Unified Air-Sea Interface for Fully Coupled Atmosphere-Wave-Ocean Models for Improving Intensity Prediction of Tropical Cyclones

Annual Progress Report 2012

PI: Shuyi S. Chen
Rosenstiel School of Marine and Atmospheric Science
University of Miami
4600 Rickenbacker Causeway, Miami, FL 33149
Phone: (305) 421-4048 FAX: (305) 421-4696 E-mail: schen@rsmas.miami.edu

Co-PIs: Mark A. Donelan and Ashwanth Srinivasan, RSMAS/University of Miami
Rick Allard, Tim Campbell, and Travis Smith, Naval Research Lab, Stennis Space Center
Sue Chen, Hao Jin, Shouping Wang, and James Doyle, Naval Research Lab, Monterey
Ralph Forster, APL/University of Washington
John Michalakes, NCAR/MMM
Hendrick Tolman, NOAA/EMC

Award Number: N00014-10-1-0162
<http://orca.rsmas.miami.edu>

LONG-TERM GOALS

The goals of this PI team are to understand the physical processes that control the air-sea interaction and its impact on rapid intensity changes in tropical cyclones (TCs), and to develop a physically based and computationally efficient coupling at the air-sea interface that is flexible for use in a multi-model system and portable for transition to the next generation research and operational coupled atmosphere-wave-ocean-land models.

OBJECTIVES

The main science and technology development objectives are to

- develop a unified air-sea interface module for fully coupled atmosphere-wave-ocean modeling systems with a general coupling framework that can transition from research to operations,
- develop new air-sea coupling parameterizations of the wind-wave-current interaction and sea spray effects and implement them in the unified module,
- implement the unified module into both research and operational coupled model systems,
- examine and constrain the budgets of momentum and enthalpy fluxes as well as the energetic balance of the fully coupled system,
- explore new physics in wind-wave-current coupling at the air-sea interface including wave-breaking and spray and bubble processes using both field observations and the air-sea wave tank at UM,
- test the generality of the air-sea interface coupling and sensitivity to physical parameterizations in the atmosphere boundary layer (ABL) and the ocean mixed layer

(OML) in the extreme wind conditions of TCs with multi-model components in the coupled modeling systems,

- evaluate and validate the coupled modeling systems in relatively data rich regions of the Gulf of Mexico and US coastal regions where data are collected regularly by the NOAA research and operational aircraft missions, and through the ONR-supported field programs over the West Pacific (i.e., TCS-08 and ITOP), and
- demonstrate the utility of the newly developed air-sea interface module for improving TC intensity forecasts in real-time.

APPROACH AND WORK PLAN

The development of the unified air-sea interface module has been consistent with the proposed scientific and technical approaches over the last three years. The focus is to develop and test the air-sea interface module in a multi-model, fully coupled framework that is general and flexible for future transition and applications in research and operational models. To ensure the generality and utility of the unified air-sea interface module, two models from each component, i.e., the atmosphere, the surface waves, and the ocean are included in the development. The current component models are COAMPS, WRF, NCOM, HYCOM, SWAN and UMWM. The NOAA WAVEWATCH III is the third wave model that will be included in the coupled system. One of the goals is to make the transition of the air-sea coupling parameterizations developed under this project and others in the community to the operational coupled models. We will continue to take advantage of the recent advancement in the applications of the Earth System Modeling Framework (ESMF) Version 5 in the multi-model system.

One of the most critical components in the air-sea interface module is the energy balance. Coupling at the air-sea interface with surface waves is essential, which needs the level of flexibility and computational efficiency that current wave models are lacking. To address issues related to computational efficiency, a new wave model has been developed. Shuyi Chen and M. Donelan have been working with a graduate student Milan Curcic at RSMAS in developing and testing the new UMWM. A. Srinivasan works in collaboration with Chen at RSMAS and scientists at NRL-SSC on HYCOM related data assimilation and ESMF capabilities. R. Allard leads the efforts at NRL-SSC in wave-ocean coupling using SWAN and NCOM. He and T. Smith work with their colleagues at NRL-MRY on testing new air-sea physical parameterizations in COAMPS-TC. Sue Chen is responsible for the overall development related to COAMPS-TC. She works closely with her colleagues at NRL-MRY (H. Jin, S. Wang and J. Doyle) and NRL-SSC on the implementation of new air-sea interface module in COAMPS-TC. T. Campbell of NRL-SSC, J. Michalakes of NCAR, and H. Tolman of NOAA/EMC are responsible for the ESMF implementation and testing the interface module in the coupled modeling system.

The PI team of the NOPP project has met in March 2012 at RSMAS/UM. The meeting summary has been posted on the NOPP website at <http://www.nopp.org/2012/national-oceanographic-partnership-program-nopp-tropical-cyclone-principal-investigators-meeting-at-the-university-of-miami-1-2-march-2012/>

The work completed during the third year is summarized in the following sections. The work plan for the remaining FY13 will be: 1) to improve the unified air-sea interface physics, 2)

investigating how surface gravity waves modify the momentum flux to subsurface currents via three mechanisms (the Coriolis-Stokes effect, the air-sea momentum budget, and the wave-current interaction), 3) to complete the implementation of the unified air-sea interface based on the NUOPC interoperability software layer, and 4) summarize the results in publications and assisting transition the outcome to community research and operational models.

WORK COMPLETED

During the third year of this NOPP project (November 2011-October 2012), the PI team have completed the following tasks: 1) implementation of the unified air-sea interface using ESMF and a common exchange grid for all component models in the coupled model systems; 2) University of Miami Wave Model (UMWM) has been integrated into COAMPS-TC and UMCM, which demonstrate the interoperability of the coupling systems; 3) both coupled modeling systems have been tested and evaluated in Hurricane Isaac (2012) with in situ surface and upper ocean observations, 4) integration of the 2011 atmospheric physics upgrade from the uncoupled COAMPS-TC into the coupled 2012 COAMPS-TC version; 5) assimilation of AXBT data in COAMPS-TC with NCODA in Tropical Storm Emily (2011) and Isaac (2012); 6) integrated ESMF interface layer for Wavewatch III into the latest development version; 7) updated Wavewatch III ESMF interface layer to use the NUOPC conventions; and 8) improved ITOP dropsonde data analysis and calculations of air-sea momentum, heat, and moisture fluxes for coupled model evaluation and verification.

RESULTS

1. Unified Air-Sea Interface

Prototype air-sea interface module approaches have been successfully implemented in both COAMPS and UMCM. Interoperability is demonstrated through the integration of UMWM into both systems. Significant progress has been made towards development of a single air-sea interface coupling infrastructure that is based on the National Unified Operational Prediction Capability (NUOPC) ESMF interoperability software layer. The interoperability software layer consists of a collection of generic code and a catalog of very specific technical rules. The technical rules form the underpinning of a common model architecture, while the generic code collection implements the rules and provides tangible pieces of software. The NUOPC/ESMF software modules are now available for developing coupled application drivers, model components and the couplers that transform data between components. The NUOPC/ESMF based unified air-sea interface coupling software profits from the benefits of increased interoperability and compatibility checking. Development of an independent grid approach in the air-sea interface component will be completed during the next several months, which will enable full interoperability of model components and the air-sea interface module.

The PIs from UM, NRL-SSC and NRL-MRY have conducted a number of fully coupled atmosphere-wave-ocean model forecasts of tropical cyclones in the West Pacific – Typhoon Fanapi (2010) observed in ITOP and recent Atlantic tropical storms and hurricanes including Hurricane Isaac (2012).

2. Coupled Model Experiments with the Unified Air-Sea Interface

The University of Miami Wave Model (UMWM, Donelan et al. 2012) has been integrated into both COAMPS-TC and UMCM to facilitate the unified air-sea interface development and continued improvement. UMCM calculates the directional wind-wave (form) stress on the waves and adds the vector form stress to the sheltering-modified skin stress similar to that of Chen et al. (2012). The resulting drag coefficient versus wind speed is shown to have the observed structure – low in light winds; increasing in moderate winds; and leveling out to a limiting value in very strong winds. UMCM has been extensively tested in real-time forecast mode from July-September 2012. The model is evaluated and verified with in situ observations from the NDBC buoys and surface Met drifters deployed during the Consortium for Advanced Research on Transport of Hydrocarbon in the Environment (CARTHE) field campaign that covers a wide range of weather conditions from calm winds to extreme winds in hurricanes.

Examples of the UMCM forecasts of Tropical Storm Debby and Hurricane Isaac show that the coupled model can improve forecasts not only intensity but also storm tracks in these cases. Fig. 2.1 shows UMCM real-time 5-day forecasts initialized 0000 UTC daily from 23-28 June 2012. Forecasts are compared with the NHC best track data and the NOAA operational models including GFS, HWRF and GDFL.

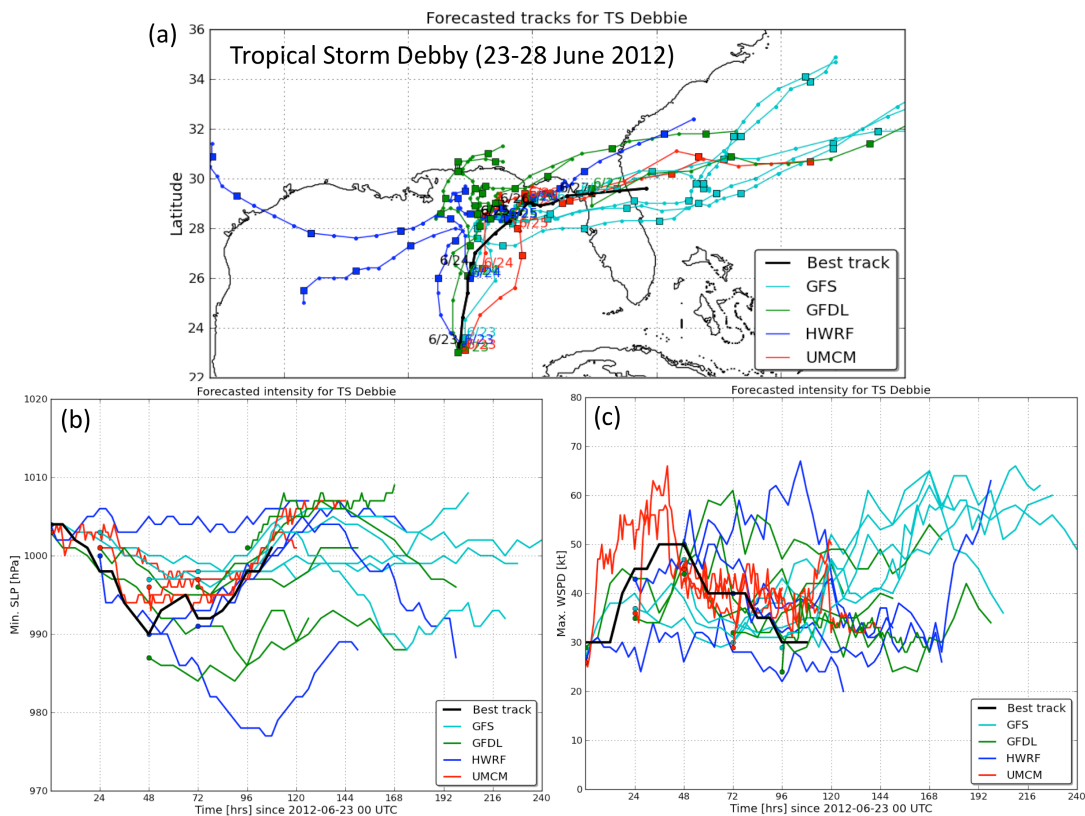


Fig. 2.1 UMCM forecasts (red) of TS Debby from 23-28 June 2012 compared with the NHC best track (black), GFS (cyan), GFDL (green), and HWRF (blue): (a) tracks, (b) MSLP, and (c) maximum wind speed. The models are initialized at 0000 UTC daily from 23-28 June 2012.

We have conducted a number of model experiments to better understand the coupled model physics compared with that of uncoupled model. Figs. 2.2 and 2.3 show the comparisons of uncoupled atmosphere (WRF), coupled atmosphere-ocean (WRF-HYCOM), and fully coupled atmosphere-wave-ocean (WRF-UMWM-HYCOM) models. The coupled models have a better track forecasts compared to the uncoupled model (Fig. 2.2), largely due to the fact that coupled model captured the asymmetric structure of Hurricane Isaac, whereas the uncoupled model over-predict storm intensity with a stronger and more symmetric storm (Fig. 2.3). UMCM is configured in multi-nested grids with 12-, 4-, and 1.3-km grid resolutions.

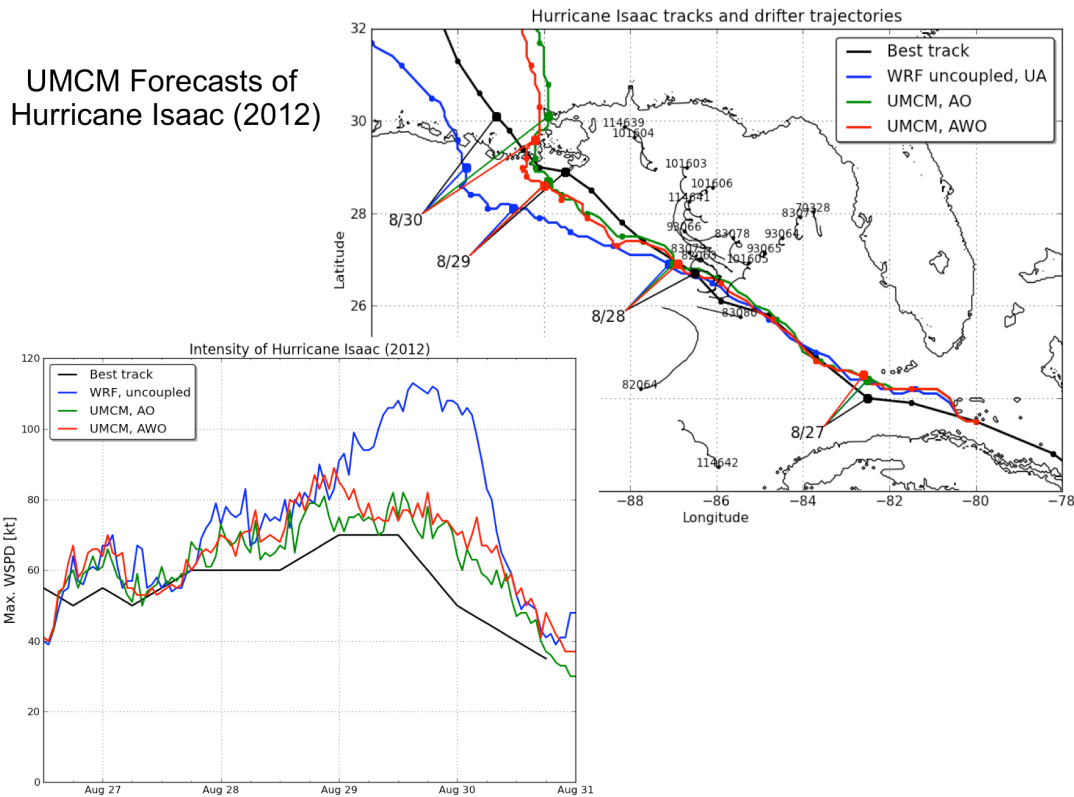


Fig. 2.2 Model forecasts (uncoupled UA-blue, coupled AO-green, and fully coupled AWO-red) of Hurricane Isaac (initialized at 1200 UTC 26 August 2012) compared with the NHC best track (black): storm tracks (top right) and maximum wind speed (bottom left). Locations of surface and subsurface ocean drifters are shown in the top panel.

Multiple field campaigns took place in the Gulf of Mexico during Isaac, including the CARTHE GLAD supported by GoMRI and ONR AXBTs deployment program. Many ocean drifters and AXBTs were deployed, which provided unprecedented surface and upper ocean data for coupled model verification. Here we present some examples of comparisons of coupled model forecasts and ADOS surface data (Fig. 2.4) and subsurface temperature (Fig. 2.5) on the right side of Isaac track. The ADOS drifters were deployed by the Air Force 53rd C-130 aircraft in collaboration with scientists from Scripps Institute of Oceanography. The ABXT data is provided by Dr. E. Sanabia of USNA (Fig. 2.6).

UMCM Forecasts of Surface Wind Speed and C_D in TS Issac (1200 28 Aug 2012)

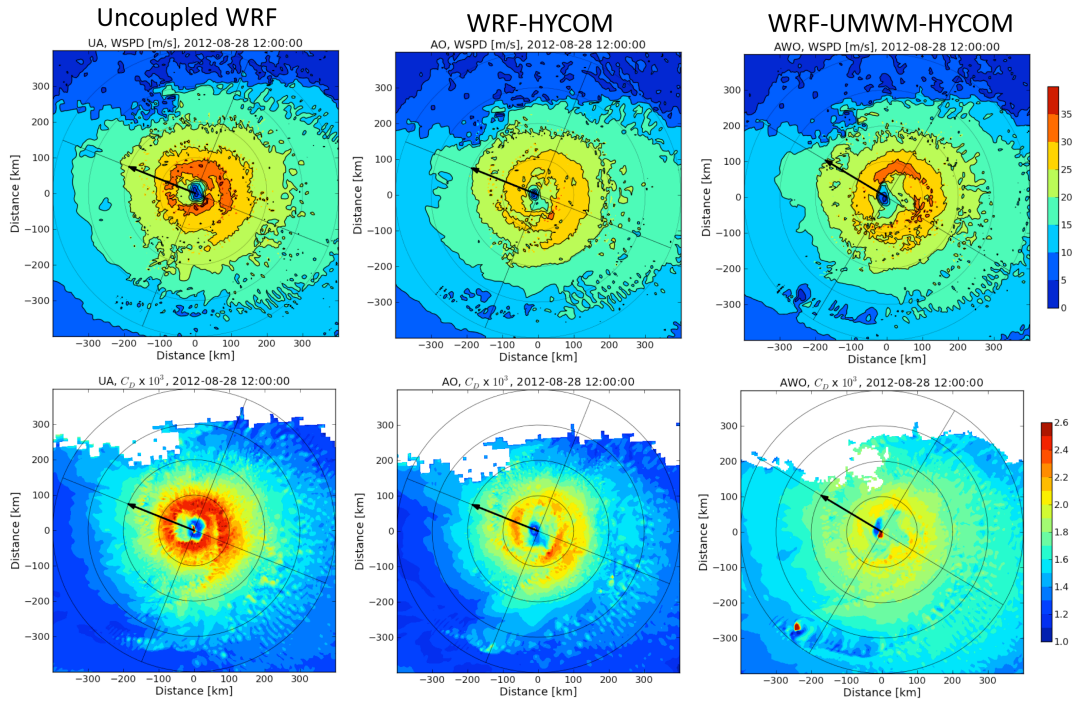


Fig. 2.3 Model forecasts of surface wind speed and drag coefficient from the uncoupled UA (WRF), coupled AO (WRF-HYCOM), and fully coupled AWO (WRF-UMWM-HYCOM) in Hurricane Isaac at 1200 UTC 28 August 2012.

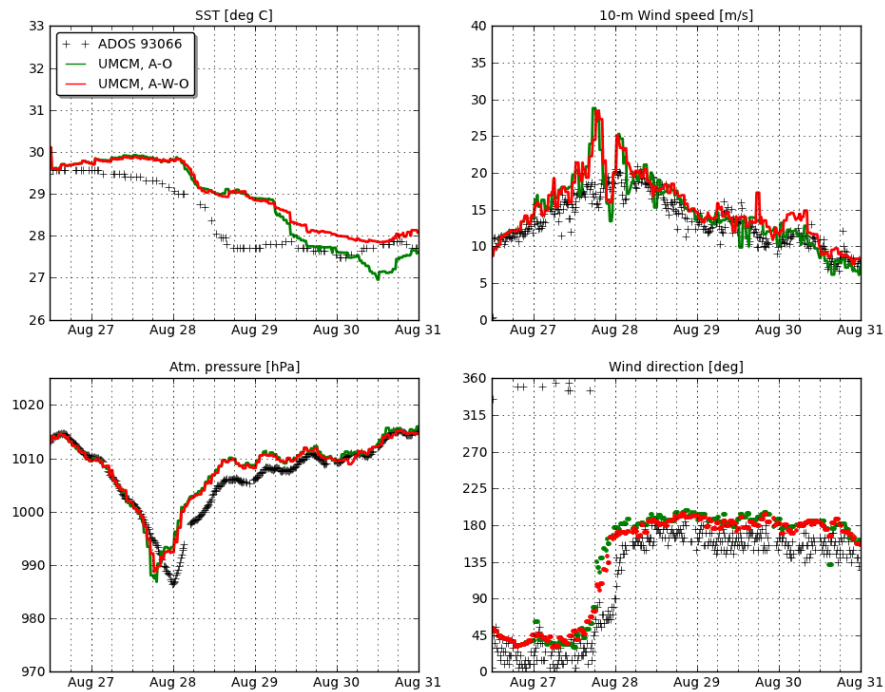


Fig. 2.4 ADOS drifter observed (black) and UMCM model forecasts (AO-green, AWO-red) of SST, sea level pressure, surface wind speed and direction.

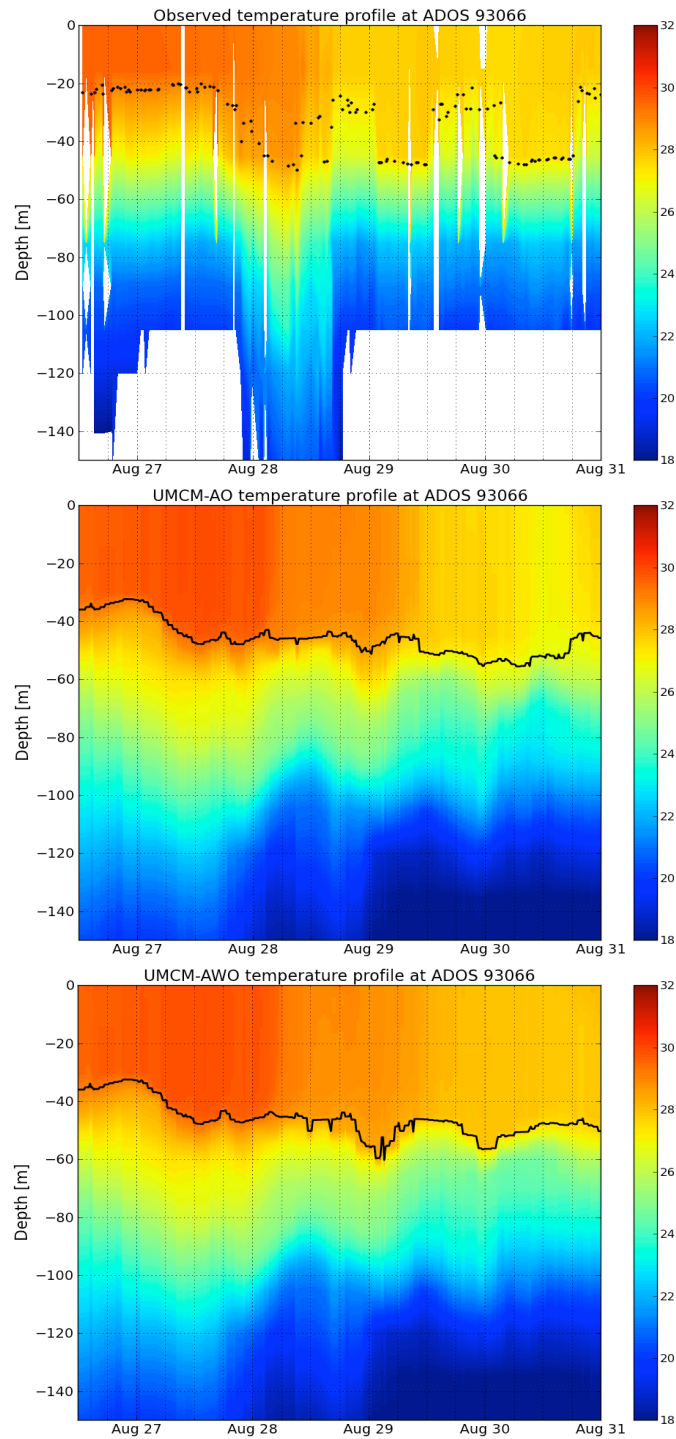


Fig. 2.5 Time series of ADOS drifter observed (top) and UMCM model forecasts (AO-middle, AWO-bottom) of upper ocean temperature from 0-150 m from 1200 UTC August 26-0000 UTC August 31, 2012. Mixed layer depth is marked in black dots/lines.

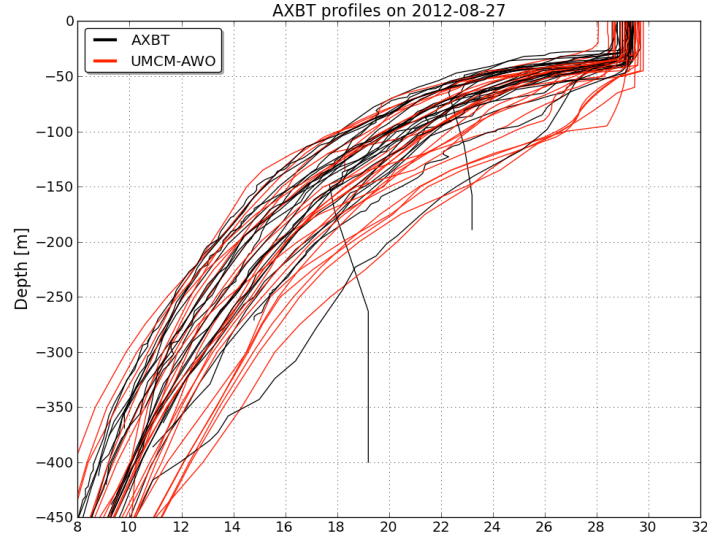


Fig. 2.6 Upper ocean temperature profiles observed by AXBTs deployed on 27 August 2012 (black) and the UMCM forecast (red).

Although the general characteristics of the upper ocean temperature is similar between the coupled model forecast and AXBT data, it is evident that HYCOM is warmer with slightly deeper mixed layer than the observations (Figs. 2.5 and 2.6).

3. Advanced wave-ocean coupling in tropical cyclones

1) Stokes drift current and TKE production

The Stokes' Drift current profile generated from the SWAN wave frequency spectrum is utilized in NCOM in four ways following Kantha and Clayson (2004):

- in the Coriolis terms of the NCOM momentum equations
- in the continuity equation
- for advection of the momentum and scalar field
- for shear production terms in the turbulent kinetic energy (TKE) and turbulent length-scale equations.

Stokes' production of TKE is computed from the vertical shear of the Stokes' Drift Current and shear stress of the Eulerian current:

$$P_{ST} = -\rho \overline{uw} \frac{\partial U_E}{\partial z} - \rho \overline{vw} \frac{\partial V_E}{\partial z}. \quad (1)$$

The shear stress is computed from the vertical shear of the current:

$$\overline{uw} = -K_m \frac{\partial U}{\partial z}; \quad \overline{vw} = -K_m \frac{\partial V}{\partial z} \quad (2)$$

Substituting, the Stokes' production of TKE calculated in NCOM is the following:

$$P_{ST} = K_m \left(\frac{\partial U}{\partial z} \frac{\partial U_z}{\partial z} + \frac{\partial V}{\partial z} \frac{\partial V_z}{\partial z} \right) \quad (3)$$

where K_m is the eddy viscosity determined from the turbulence closure model (Kantha and Clayson (2004)). In the TKE equation, the Kantha and Clayson (2004) parameterization scales K_m to a value of 7.2 for the Stokes' Drift shear production term versus the normal scaling factor of 1.8 for the normal shear production term. When SDC is present, a significant increase in the turbulent length scale will occur and significantly increase mixing in the upper ocean.

Early studies of the SDC assumed that the SDC vectors are mostly aligned with the surface wind stress vectors; however, extreme situations such as a tropical cyclone (TC), tend to produce a large misalignment angle between these vectors. The misalignment of both wind and waves is important to understanding the dynamics of Langmuir turbulence (LT) on the mixed layer, especially in the context of TCs. The wind/wave field is extremely complex in tropical cyclones, especially since the TC produces a wave field that contains both large swell and wind waves. Propagating swell waves in particular are susceptible to misalignment with the wind direction as well as quick changes in wind direction associated with TCs. Recent studies show that greater misalignment decreases the generation of LT and it has been hypothesized that in extreme cases when the SDC directly opposes the wind stress, there is minimal generation of LT (Van Roekel et al. 2012). There are no modeling studies currently published discussing these concepts in the context of a tropical cyclone.

Example: Hurricane Ivan (2004)

Hurricane Ivan, generated in a fully-coupled air-ocean-wave COAMPS-TC simulation, is translating to the north at about 10 kts in Fig. 1. The eyewall, denoted as a circle in Fig. 1, shows that the misalignment angle between the SDC and wind stress within the core of the hurricane approaches 180 degrees on the left flank relative to the spatial translation. This misalignment angle, as shown in the idealized study of Van Roekel et al. (2012) (not in terms of a tropical cyclone) works to inhibit upwelling/downwelling. The large misalignment angle in Hurricane Ivan (Point A) occurs where surface wind speeds within the eyewall are greater than 50 m s^{-1} and wave heights are in excess of 10 m. In terms of upper-ocean shear production of TKE and mixing in the same misalignment angle region, calculations of the shear term in Eq. 3 yield interesting results. A simple grid point calculation of the vertical shear terms (surface to 10 m depth) in Eq. 3 at each forecast hour at points A and B is shown in Table 1. At Point A, the Stokes' shear production term becomes very small at forecast hour 42 and even changes sign at forecast hour 43 at the time of greatest misalignment angle. A negative contribution to the total shear production of TKE implies that the inclusion of the SDC at this particular time may actually *decrease* mixing in the left flank relative to the spatial translation. Nevertheless, the small Stokes' shear production TKE terms at point A compared to point B in the right flank of the eyewall implies that there is less mixing occurring at point A than at point B, given that the magnitude of the wind stress is similar at both locations within the nearly axisymmetric eyewall.

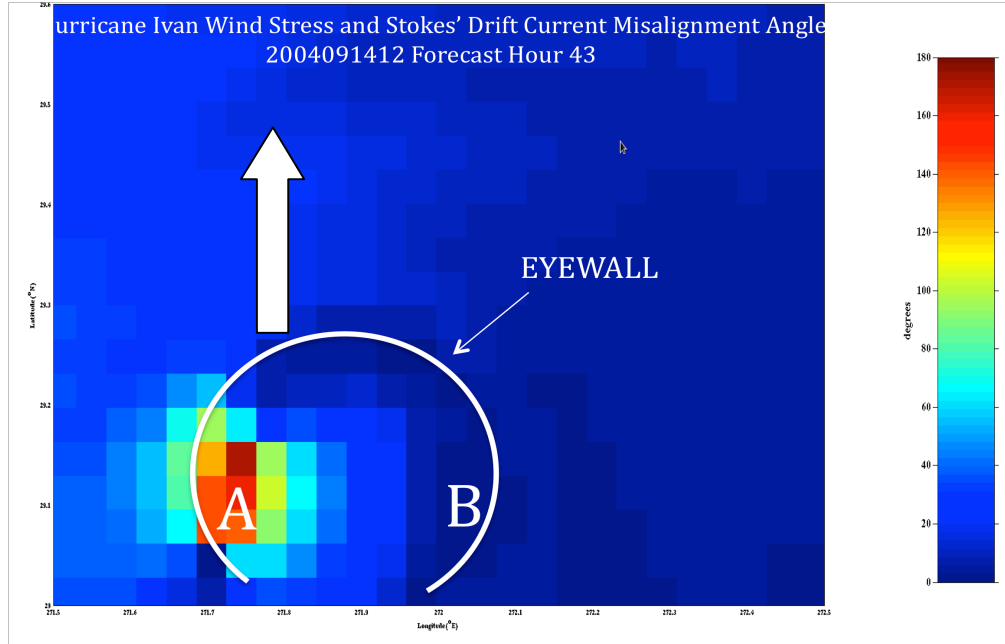


Fig. 1: Misalignment angle (degrees) between the surface wind stress vectors and surface Stokes' drift current vectors. The eyewall of Hurricane Ivan is denoted by the circle. The translation direction and speed is north at 10 kts.

Hurricane Ivan (Stokes' drift shear production term in TKE equation)			
Forecast Hour	left eyewall ($\times 10^{-4}$) (point A)	right eyewall ($\times 10^{-4}$) (point B)	Point A θ_m
38	7.4	7.4	14.5
39	8.5	8.2	12.1
40	9.0	7.9	10.8
41	9.0	7.6	13.4
42	1.9	7.6	1.2
43	-0.5	8.9	142.0
44	6.4	7.5	15.3
45	6.3	7.3	4.9
46	5.8	6.1	4.2
47	5.2	4.9	1.1
48	4.6	4.6	0.3
49	4.2	2.7	0.5
50	3.0	2.3	2.3

Table 1: Magnitude of the Stokes' drift shear production term in the TKE equation (Eq. 3) at points A and B in Fig. 1 for each forecast hour 38-50. The TKE shear production term at point A is negative at hour 43 at the time of greatest misalignment angle.

2) Hurricane Isaac in COAMPS-TC

Atmosphere-only (A-only), atmosphere-ocean (AO), and atmosphere-ocean-wave (AOW) simulations of WRF/HYCOM/UMWM and COAMPS-TC models were both tested with similar resolutions (COAMPS-TC setup below) for Hurricane Isaac that developed in the

Caribbean Sea and entered the Gulf of Mexico in late August 2012. A plethora of ocean observational data including drifter profilers and AXBTs sampled the upper ocean as Isaac traversed the Gulf of Mexico. Also, NOAA wave buoys provided useful SWH information for the simulations including the wave model.

Similar to the WRF/HYCOM/UMWMM model setup, the COAMPS-TC model setup for Hurricane Isaac (Fig. 2) consists of a triple-nested atmospheric domain with 18, 6, and 2 km horizontal resolution (12, 4, and 1.3 km in UM model) and a total of 60 terrain-following vertical levels. The outer, coarse nest extends from the equator to 38°N and from 65°W to 108°W, with horizontal dimensions of 250 × 250. The two inner nests translate in tandem with the cyclone's vortex center. Atmospheric boundary conditions are provided by the Navy Global Atmospheric Prediction System (NOGAPS) model. The TC vortex initialization in NAVDAS is enabled through a TC warning message that includes location, wind radii (distance of a certain wind speed threshold from the center of circulation), and intensity information provided by the National Hurricane Center in Miami, FL and the Joint Typhoon Warning Center in Hawaii. Each data assimilation cycle is initiated using the prior 12-hour forecast as background, incorporating quality-controlled observations from radiosondes, aircraft, satellite, ship, and surface stations.

The NCOM configuration (Fig. 2) consists of one nest (4 km resolution, same as HYCOM in UM model) that encompasses the GOM and the Caribbean Sea. This ocean nest extends from 10°N to 31°N and from 67°W to 98°W, with horizontal dimensions of 800 × 600. A total of 50 vertical levels, 36 of which are sigma coordinate levels in the upper 190 m of the water column, are used with the Navy's Digital Bathymetric Data Base (DBDB2) data set. NCOM is initialized using global NCOM hindcast data. NCODA 3DVAR ingests observational and global model ocean data including quality-controlled satellite, ship, and profiler data for each update cycle. The ocean model is run with tides and rivers included.

The SWAN model configuration consists of one nest (8 km resolution (4 km in UM model)) that encompasses the exact latitude and longitude domain of the NCOM ocean nest, with horizontal dimensions of 400 × 300. Thirty-six discrete directions and 25 frequency bands are selected for use with the same DBDB2 bathymetry. Boundary conditions for SWAN would normally consist of energy spectra from a larger global model, such as WAVEWATCH III (WW3). Since the TC generates the dominant wave contributions to the wave field and the GOM is a semi-enclosed sea, the boundary conditions for SWAN were not prescribed in these simulations.

The ocean and wave models provide feedback to the atmosphere through the high-resolution NCOM SSTs and SWAN wave age (Moon et al. 2004b), which is computed from SWAN wave spectra. The SWAN wave age is used to formulate the Charnock relation for the atmospheric model to improve atmospheric heat and moisture fluxes in TC conditions. The TC intensity is sensitive to ocean and wave model feedback to the atmosphere (Chen et al. 2010; Halliwell et al. 2011). In this study, the interactions between NCOM and SWAN were explored through both coupled and uncoupled Hurricane Isaac simulations, while ocean and wave model feedback to the atmosphere provided an acceptable Hurricane Isaac intensity throughout the forecast track, until just before landfall when the intensity was too high.

Hurricane Isaac was a tropical storm in the eastern and central GOM from 26-28 August, only becoming a hurricane shortly before landfall on the 28 August 2012. Spin-up of COAMPS-TC with 12-hour atmosphere and ocean data assimilation cycles commenced at 0000 UTC 20 August. Hurricane Isaac's vortex was initialized on 0000 UTC 25 August over the central Caribbean Sea. This spin-up provided a good initial ocean and wave state as Isaac entered the

GOM on 26 August. For all model runs, a 72-hour forecast of Hurricane Isaac was generated at 1200 UTC 26 August to provide comparisons to in-situ ocean and wave observational data.

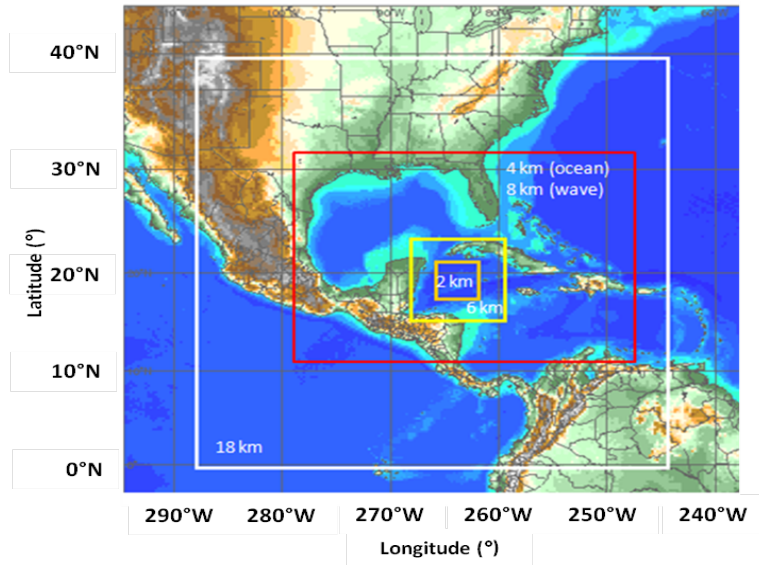


Fig. 2: Atmospheric (18 (white), 6 (yellow), and 2 (orange) km) and ocean/wave (4/8 km, red) nests setup for Hurricane Isaac. The 6 and 2 km inner atmospheric nests move in tandem with the TC center. The ocean and wave nests are large to allow for appropriate numerical spin-up of the cyclone over the Caribbean Sea before entering the Gulf of Mexico.

The 72-hour 2012082612 forecast of Hurricane Isaac using 0.5 degree NOGAPS boundary conditions produced a good, but similar forecast track for the A-only, AO, and AOW simulations. Although the track is very good, the timing is too quick for landfall near the end of the 72-hour forecast (Fig. 3).

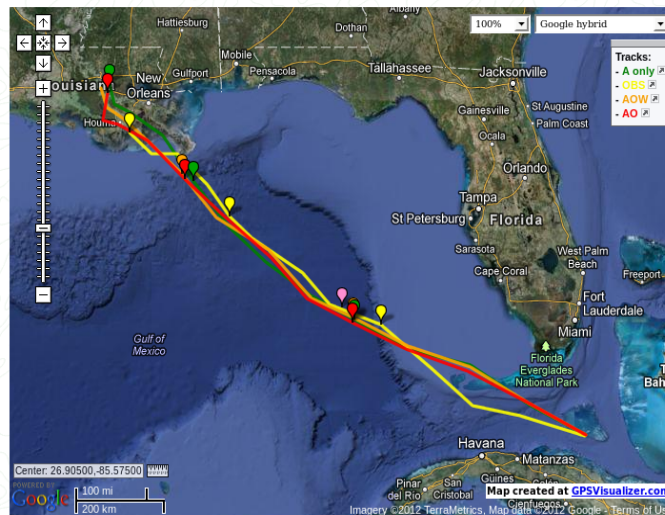


Fig. 3: Track of Hurricane Isaac for 2012082612 72-hour forecast over the Gulf of Mexico. Isaac is initialized between the Florida Straits and Cuba at 0000 UTC 2012082612. Tracks for the A-only (green), AO (red), AOW (orange) and observations (yellow) are shown. Widgets indicate the positions of Isaac after 24, 48, and 72 hours, respectively.

The intensity of Hurricane Isaac for each of the simulations is shown in Fig. 4. Isaac was rather disorganized throughout most of the TC's life cycle due to land interaction, 10-15 kts of vertical wind shear, and mid-level dry air intrusion that consistently disallowed eyewall formation even though SSTs were very favorable. The intensity of Isaac in each of the three simulations indicate a very good agreement over the eastern Gulf of Mexico; however, the intensity of Isaac increased significantly near landfall in all three simulations, but only a modest intensity gain was observed. The addition of ocean and wave coupling to the atmosphere produces a stronger storm than the A-only simulation. However, additional tests of intense hurricanes in COAMPS-TC have indicated that AO and AOW coupling and fluxes therein are necessary to produce more realistic intensities (e.g. Hurricane Ivan in the GOM (September 2004)). Since the A-only model run in Hurricane Isaac's case produced an intensity that was too high, it is more than likely that the atmospheric model shows an atmosphere that is much more conducive for intensification than was observed.

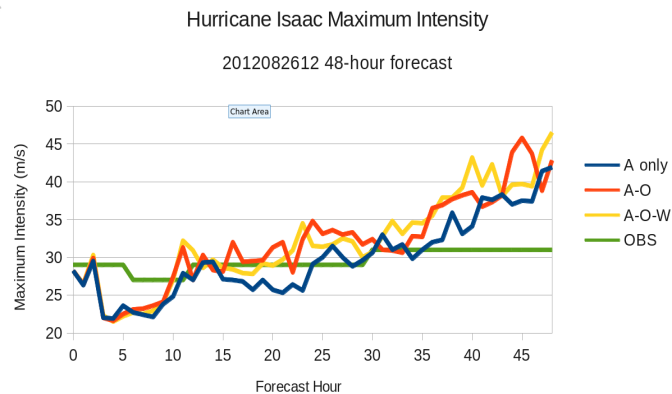


Fig. 4: Maximum intensity of Hurricane Isaac for the first 48 hours of the 2012082612 72-hour forecast. Landfall occurs shortly thereafter.

A snapshot of the wind field for each of the three simulations show that the addition of AO and AOW coupling produces more vigorous convection within the eyewall than in the A-only case. The increased organization of convection, especially in the AOW case, allowed for Isaac to become quite intense before landfall in the AOW simulation (Fig 5).

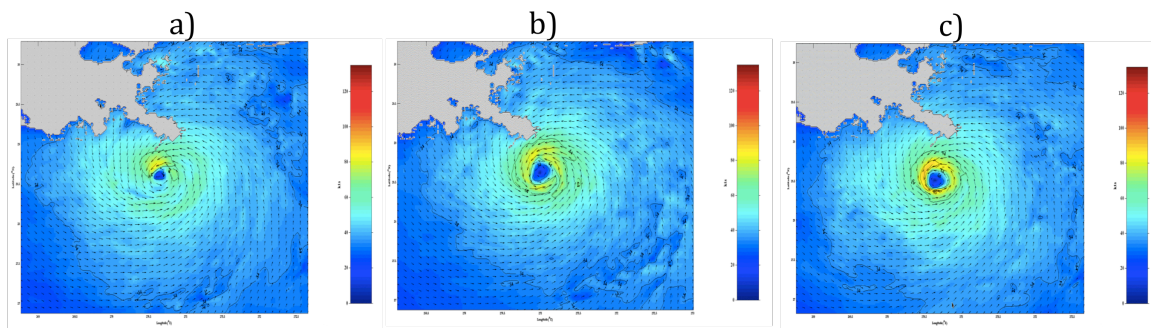


Fig. 5: Snapshots of Hurricane Isaac near landfall of the a) A-only, b) AO, and c) AOW 10-m wind field.

A few AOW model run comparisons of ADOS drifter profiles and AXBTs were produced to analyze the upper 125-150 m of ocean before and after the passage of Hurricane Isaac over the GOM. Most of the drifter vertical temperature profiles and AXBT vertical temperature profiles comparisons were quite good before and after Isaac, i.e., the depth of the mixed layer and extent of the thermocline had a tendency to agree in the AOW simulation.

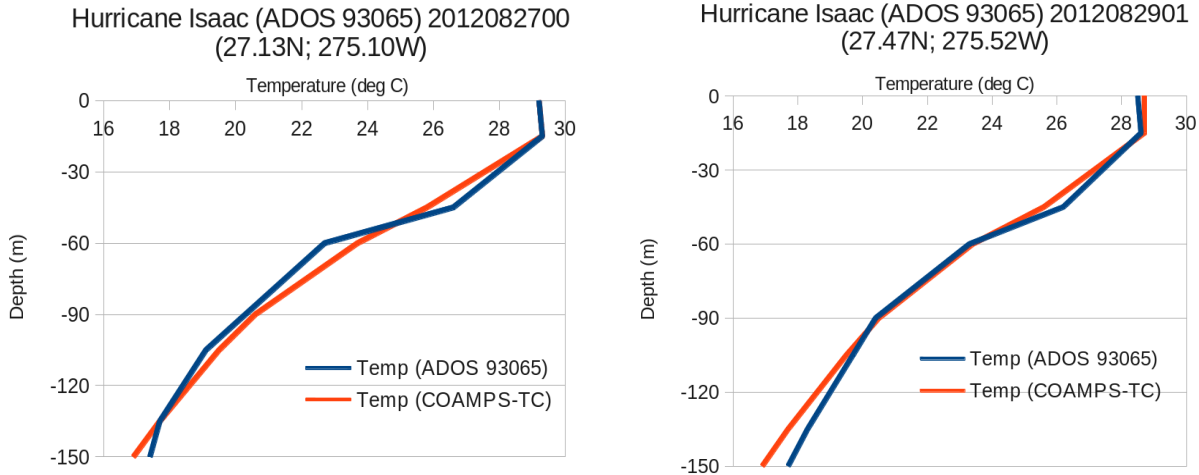


Fig. 6: 2012082700 (left: before Isaac) and 2012082901 (right: after Isaac) ADOS 93065 drifter and COAMPS-TC vertical temperature profile comparisons.

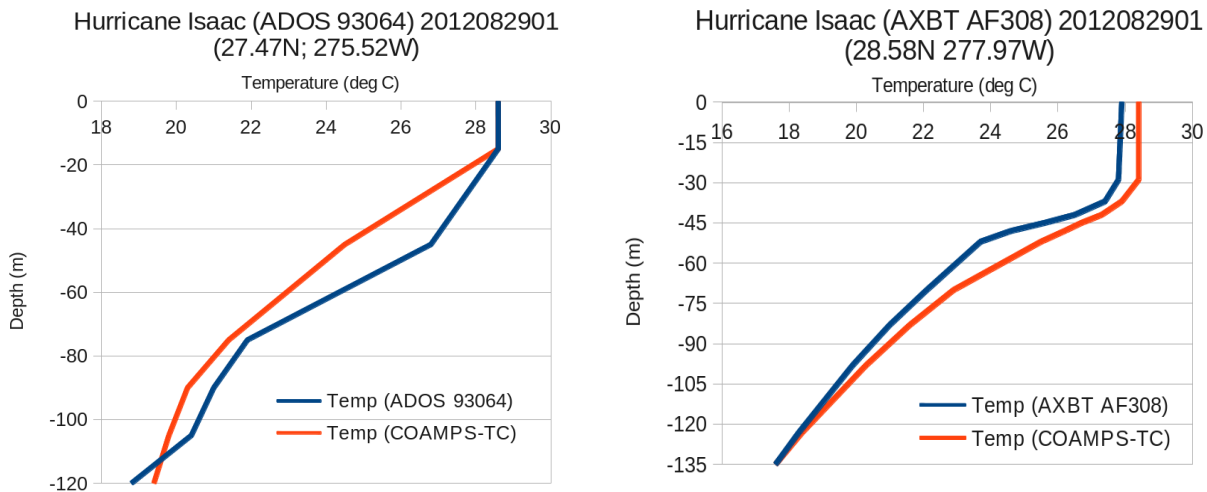


Fig. 7: 2012082901 (after Isaac) vertical temperature profile comparisons for ADOS 93064 drifter (left) and AXBT AF308-5 (right).

The NOAA Buoy 42003 in the eastern GOM was directly within the path of Hurricane Isaac. A comparison of the AO (now ocean to wave feedback) and AOW simulations is shown in Fig. 8. Although the SWH prediction was too high in both the AO and AOW simulations compared to observations, the addition of ocean to wave coupling (i.e., passing NCOM currents to SWAN) produced a lower maximum SWH at Buoy 42003. The passing of NCOM surface currents and water levels to SWAN is important for several reasons. Water levels can modify the water depth utilized within the wave model physics calculations. However, this modification will, at most, add only a few meters to the overall water depth used in SWAN, especially in deep

waters. More importantly, surface currents ingested by the wave model alter the effective wind speed (i.e., wind speed relative to a frame of reference moving with the currents) and horizontal shear in the currents produces changes to wave length, height, and direction in a manner similar to refraction and shoaling by interaction with variable bathymetry. In general SWH could be reduced as much as 1-3 meters when ocean currents are passed to SWAN in high-wind TC conditions.

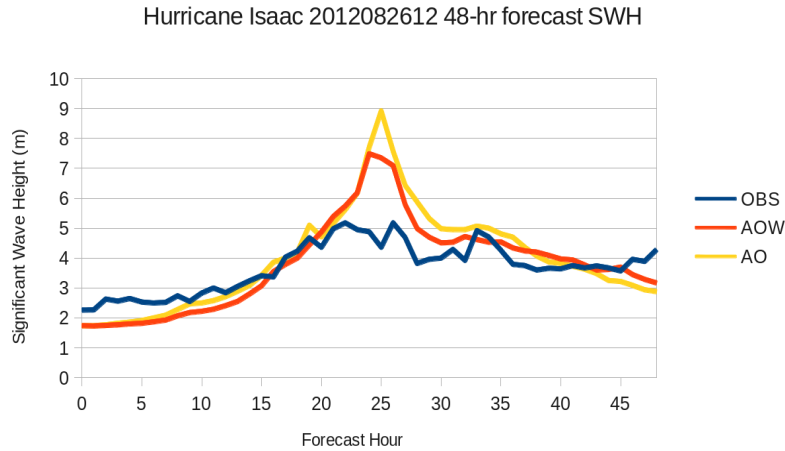


Fig. 8: SWH for the coupled (red) and uncoupled (yellow) ocean/wave feedback AOW simulation at NOAA Buoy 42003 (blue).

The plethora of observational data for Hurricane Isaac will allow for excellent testing of the unified air-sea-interface upon completion. This data will allow for consistent and thorough testing and comparisons for both COAMPS-TC and the WRF/HYCOM/UMWM model.

4. Assimilation of AXBT data in COAMPS-TC

We integrated the 2011 atmospheric physics upgrade from the uncoupled COAMPS-TC into the coupled 2012 COAMPS-TC version. The most significant improvement seen in the uncoupled COAMPS-TC is the generalized microphysics (Schmidt, personal communication), which decreased the model tropospheric temperature bias and 3-5 days track errors. We use this new version to demonstrate the air-ocean coupled COAMPS-TC system in real-time during the 2011 Atlantic hurricane season in conjunction with the Airborne eXpendable BathyThermographs (AXBTs) demonstration project (Sanabia et al. 2012). The purpose of the AXBT project is to investigate the usefulness of AXBTs in an *operational* setting and their impact on the forecast hurricane track, intensity, and upper-ocean structure.

Two case studies were performed using the air-ocean coupled COAMPS-TC. A data denial experiment of the COAMPS-TC model revealed the impact of the AXBT data on the upper-ocean thermal structure. The first case samples the warm core ring (WCR) structure in the Gulf of Mexico. The AXBTs were deployed across the center of this WCR during the training flight. Inclusion of the AXBT data in the COAMPS-TC NCODA assimilation resulted in the reduction of the temperature in the center, northeast, and northwest edges of the WCR by up to 1.5°C and the warming of the fringes of the WCR by up to 0.5°C.

The second case study performed is for hurricane Emily. The intensity of hurricane Emily dropped from 45 to 30 kts between 3-5 Aug due to unfavorable environmental shear. The 1200 UTC 03 August 2011 COAMPS-TC ocean model indicated that the upper ocean in the vicinity of Emily was characterized by several relatively warm and cool regions (Fig. 1). The SSTs varied between 27°C and 31°C, with the warmest waters generally located south and east of Emily as well as between Cuba and Jamaica and west of Haiti. Ocean heat content showed similar variability, with the maximum OHC above 100 kJ cm⁻² and the remainder of the Caribbean Sea generally less than 80 kJ cm⁻². A data denial sensitivity run of COAMPS-TC without the AXBT data showed that the inclusion of AXBT data resulted in changes in SSTs between -0.15°C and +0.3°C. At 100-m depth, the AXBT observations resulted in a 0.2-0.8°C temperature increase south of Puerto Rico. A similar pattern was seen in OHC, where values were 5-15 kJ cm⁻² greater ahead of Emily, and 5 kJ cm⁻² less behind Emily. When denied the AXBTs in COAMPS-TC, the track and intensity were degraded slightly (Fig. 2) but these difference is not significant. Similar results were also seen in the AXBTs denied experiment with hurricane Irene (not shown). The track and intensity differences for hurricane Irene was smaller than Emily. The reason that coupled COAMPS-TC did not show a great sensitivity for Irene was probably due to the ocean condition underneath Irene were also sampled by the NDBC buoys located near the Carolina coast. Therefore the AXBTs did not provide added information compare to the routine moored buoys.

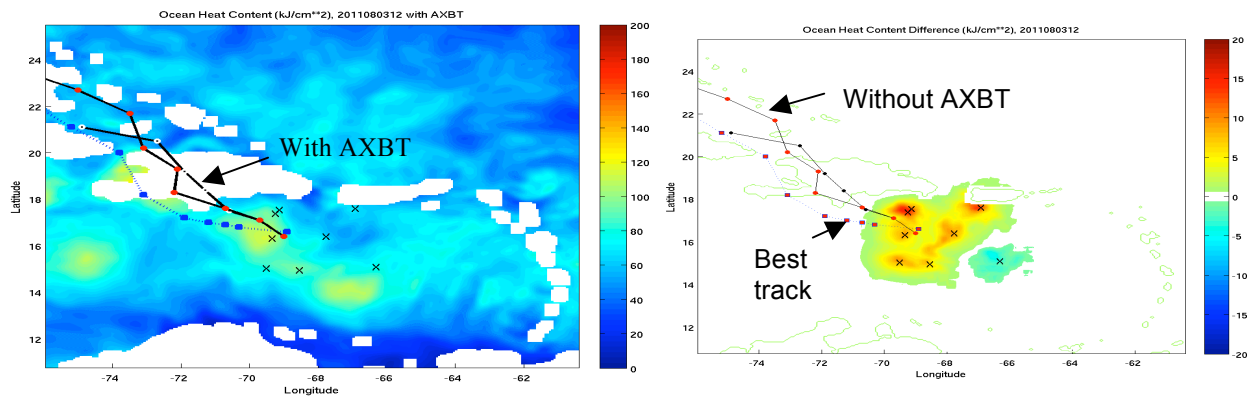


Figure 1. (a) Visible GOES-13 satellite imagery (in units of GOES VARIABLE Format (GVAR), scaled) of Tropical Storm Emily from 1245 UTC 03 August 2011. (b) Brightness temperatures (in K) from the F-17 SSMIS microwave imager at 1020 UTC 03 August 2011. Comparison of COAMPS-TC ocean heat content (OHC in kJ cm⁻²) with and without AXBTs. The numbered AXBT drop locations are denoted by black x's. The blue dashed line is the best track. COAMPS-TC track with AXBT is the black line with black dots and the track without the AXBT is the black line with red dots. The right panel shows the OHC with the AXBTs and the left panel is the OHC difference between with and without AXBTs.

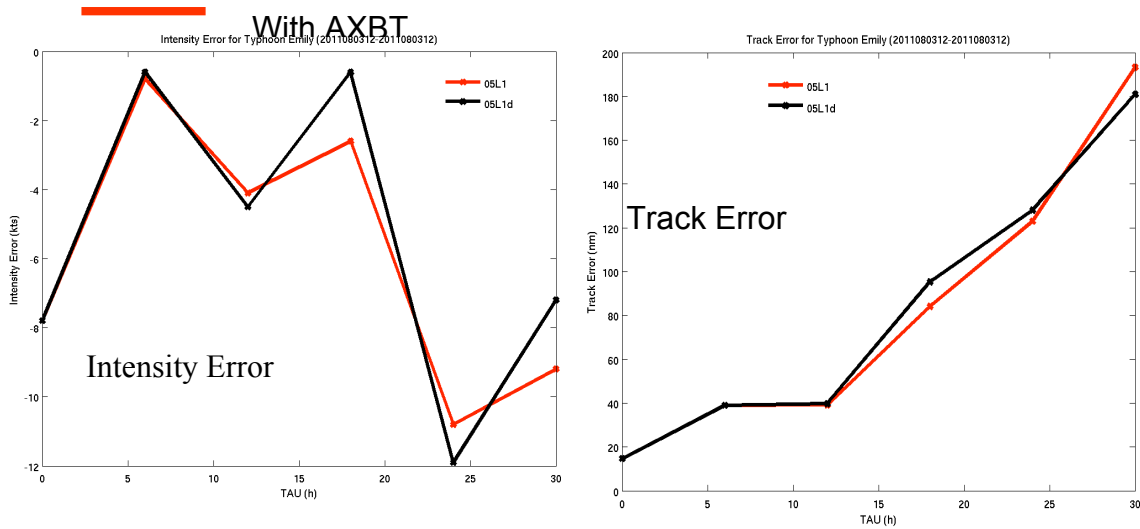


Fig. 2 Comparison of Coupled COAMPS-TC track and intensity errors for hurricane Emily. The red and black line are with and without AXBTs with respectively.

Overall during the 2011 Atlantic season, the homogeneous sample of real-time coupled COAMPS-TC from 5 storms (Irene, Katia, Maria, Ophelia, and Philippe) showed the track bias reached about 350 nautical miles by the end of five-day forecast. While the intensity was consistently lower throughout these five days. The trend of negative bias in coupled COAMPS-TC did not appear in uncoupled COAMPS-TC. The real-time uncoupled COAMPS-TC statistics showed a mean slightly over-intensification (Moskaitis, personal communication).

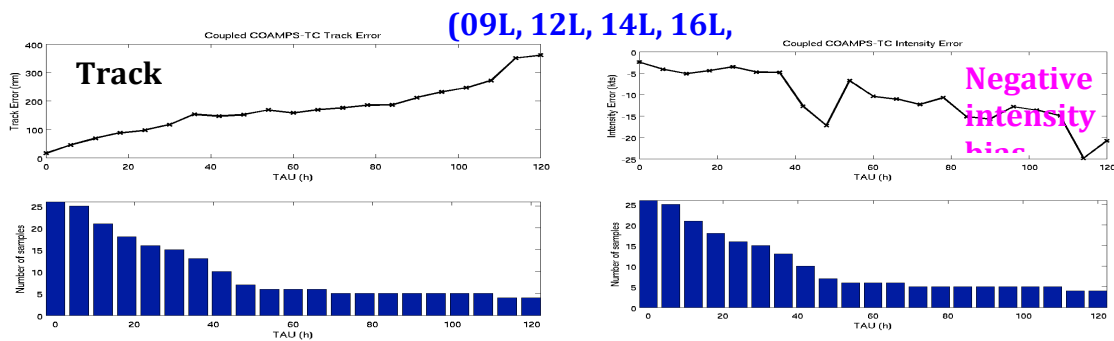


Fig. 3 Homogenous track (nautical miles, left panel) and intensity (knots, right panel) errors of air-ocean coupled COAMPS-TC for five hurricanes (Irene, Katia, Maria, Ophelia, and Philippe) during the 2011 Atlantic season. Number of sampling is shown in the bar chart at the lower panels.

To understand the source of low-intensity bias in coupled COAMPS-TC and to improve the intensity forecast, we implemented and tested a new sea spray parameterization (Fairall et al. 2009 and Bao et al. 2011) from NOAA ESRL. The test case used for this study is Typhoon Fanapi observed during the ONR Impact of Typhoon on the Upper Ocean (ITOP). Compare to

the Fairall old sea spray scheme, this new version considered the loading effect of spray particles and lower the momentum drag in higher wind speed (Bao *et al.* 2011). This effect is tested in air-ocean-wave coupled Fanapi simulation and the momentum drag was reduced from above $2.5e-3$ to as low as $1.5e-3$ for various sensitivity experiments. When capped the momentum drag to $2e-3$ or $2.5e-3$ in the AOW tests using the scalar wind-wave coupling scheme (Moon 2004 and new University of Rhode Island scheme, Ginis personal communication) that returns a sea-state dependent Charnock based on an empirical relationship of wave age and wind speed. Sensitivity runs varying the momentum drag showed the coupled COAMPS-TC maximum wind speed intensity was improved by lower the momentum drag but little change has seen in the predicted minimum sea level pressure. Domain averaged sensible and latent heat fluxes in 150 km radius from the Fanapi eye indicated lowering the momentum drag did not seem to modify much of either fluxes. Further analysis is under way to investigate the cause of intensity change.

The effect of new spray parameterization is to increase the sensible heat flux slightly and little change in the latent heat flux (Fig. 5). The averaged total flux change in the 150 km radius from the eye due to sea spray is about 5%. Even with the help of sea spray, the total flux difference between the coupled and uncoupled runs is still about 32%. There is a large discrepancy in turns of total energy transferred from the ocean to the atmosphere between coupled and uncoupled COAMPS-TC which is closely tie to the amount of induced ocean wake cooling. Work is underway to use in-situ ocean measurements to evaluate the COAMPS-TC upper-ocean forecast and to evaluate the nonlinear ocean feedback from the wind and surface wave forcing.

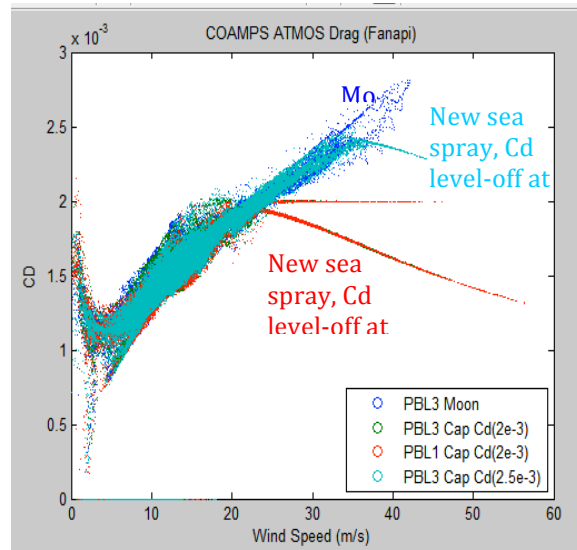


Fig. 4 Sensitivity of air-ocean-wave coupled COAMPS-TC momentum drag formulation. The blue dots are from wind-wave coupling (Moon, 2004). The green and cyan dots are Moon plus capped the momentum drag at $2e-3$ and $2.5e-3$ with respectively. The red dots are similar to green dots except the run used the original Mellor-Yamada turbulent mixing.

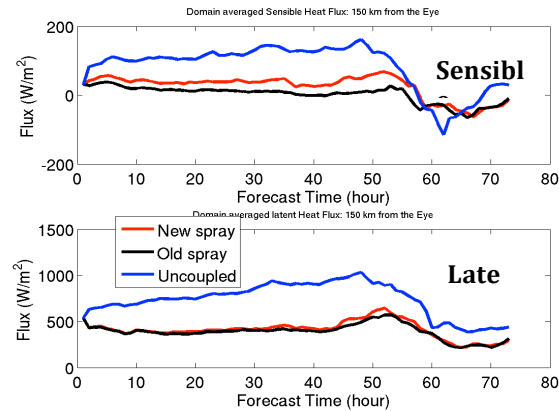


Fig. 5 Sensitivity of air-ocean-wave coupled COAMPS-TC sensible and latent heat fluxes due to sea spray.

In summary, we have seen some sensitivity of coupled COAMPS-TC with respect to the momentum drag. A new improved vector wind-wave parameterizations developed by University of Miami (Chen et al. 2012a, Donelan *et al.* 2012) is currently being implemented in coupled COAMPS-TC. We plan to test and compare this vector wind stress-wave coupling with the current scalar wind stress approach in COAMPS-TC and continue to use three test cases (Frances, Ivan, and Fanapi) to compare the 4D representation of air-ocean-wave coupled COAMPS-TC with in-situ observations.

5. Improving Dropsonde analysis for Coupled Model Evaluations

Dropsonde data are frequently the only measurements in the near-surface hurricane boundary layer. Consequently, they are used to make estimates of the surface fluxes for evaluating numerical model output. However, the data provided by dropsondes are not ideal for the purpose. We are attempting to develop means to make the estimates more rigorous.

Surface fluxes are usually estimated from drop sondes by applying standard bulk flux algorithms to sonde data interpolated to 10 m. Bulk flux models are based on Monin-Obukhov similarity (MOS), so the implicit assumption that goes into such flux estimates is that there is a layer within the sonde profile over which MOS is valid. However, MOS relates fluxes to *mean* profiles of wind, temperature and humidity. Sonde profiles must be considered to be approximately snapshot measurements of the highly turbulent boundary layer flow. That is, a single sonde profile is not necessarily representative of the mean flow and a given profile might, at first glance, appear to be quite inconsistent with MOS. It is not possible to state confidently whether or such poor agreement is due to MOS being invalid. Ideally ten or more drop sondes would be deployed simultaneously and the results averaged to produce an approximate mean flow for evaluating whether or not MOS is valid in the given case and to calculate surface fluxes. Currently, this is not possible.

An additional complication is that the estimate of the surface wind speed, which is a key parameter in bulk flux models, from drop sonde profiles is based on very precise knowledge of the sonde's location over very short time intervals. In high shear regions, such as the near-surface region of the hurricane boundary layer, the sampling rate of the GPS in the sonde is insufficient to measure velocities accurately, even though the data are frequently recorded as low as six or seven meters above the surface. The net result is that interpolated 10 m winds are not trustworthy.

Hence, we are left with two issues: the sonde winds are highly suspect in the highly-sheared near-surface region of particular interest and we have only single realizations of the flow in a very turbulent environment. From these data we must attempt to estimate the mean flow profile and the surface fluxes in order to estimate U10 and the surface fluxes.

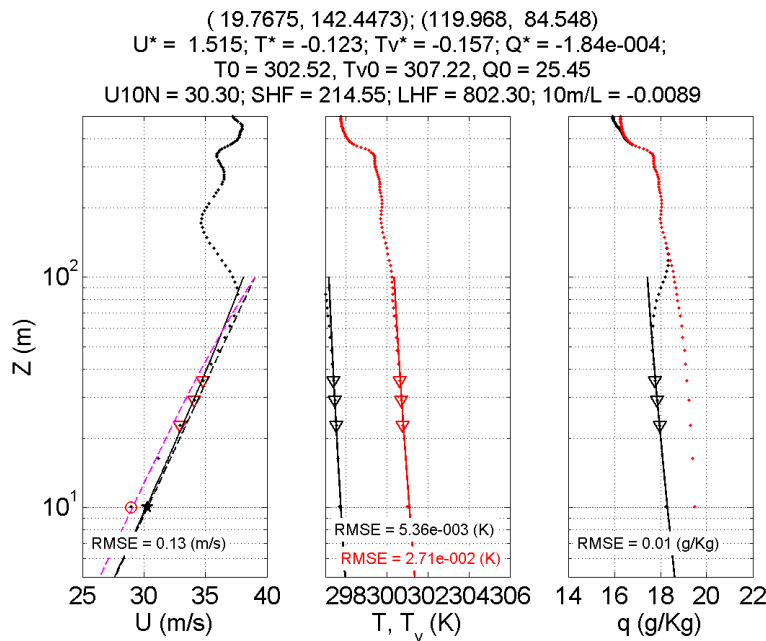


Figure 5.1 shows an example of a simple to interpret case from typhoon Malakas on September 22, 2010. The sonde data are shown as dots. The best fit MOS profiles are the solid lines and the estimated U10N, sensible heat flux (SHF) and latent heat flux (LHF) are given in the plot title. In this case, the apparent surface layer extends to about 80 m above the surface. It seems evident that averaging over the lowest 150 m of this profile will include winds that are in a different dynamical regime.

Two methods commonly for estimating U10 use the mean of the lowest 150 m of the sonde profile (U150; Franklin et al., 2003; and Uhlhorn et al. 2007). Franklin et al. (2003) analyzed eyewall profiles and fit a reduction factor that relates U150 to the surface wind as a function of the mean height of the 150 m layer used in the averaging (Z150). Sonde profiles ending as high as 180 m above the surface are used. Uhlhorn et al. (2007) made a linear fit of U10 (interpolated from the sonde profiles) to U150. They found that this was, within measurement error, equivalent to the Franklin method when Z150 ~ 85 m, which corresponds to profiles that extend to approximately 10 m above the surface. Because the parameterization is based on data from all

available flights, the inherent averaging used in the curve fit is assumed to address single-realization aspect of sonde profiles.

However, examination of profiles from ITOP calls the U150 surface wind parameterizations into some question. Quite commonly there is clear change in the slope of the wind speed profile well below 150 m that strongly suggests that the upper and lower parts profile contributing to U150 sample parts of the near surface flow that are in different dynamical regimes.

We addressed this problem from a slightly different perspective. We assume that we cannot trust sonde wind speeds at or below about 10 to 15 m above the surface. Furthermore, we assume that the dynamical regime strongly affected by the sea surface extends to approximately 50 m or so above the surface. This is a fairly conservative estimate in some cases, but inspection suggested that it does well in separating surface layer data from data that is subjected to more complex boundary layer dynamics. We further made the strong assumption that, even though the particular sonde profile represents a single realization through the turbulent flow, we can treat the measurements at different levels as being independent from each other. Instead of applying a bulk flux model to the interpolated 10 m values, we fit the implicit MOS similarity model profiles consistent with the COARE 3.0 bulk flux model (incorporating the CBLAST cap on CDN) to the wind, temperature and humidity measurements within this layer. Small corrections to the temperature to account for the radial displacement of the sonde during the drop were made. Similarly, we used the SFMR wind speeds to make small adjustments for the radial change in wind speed during the sonde descent. Neither of these corrections made significant differences in the results. When possible we used sea surface temperatures (SSTs) from co-located AXBTs. In other cases we used time- and space-interpolated SSTs from Remote Sensing Systems (RSS). This product combines microwave and IR SSTs and is produced on a 9 km grid. The RSS SSTs were generally within a few tenths of a degree with the AXBT SSTs. The model produces estimates of the MOS scaling variables U^* , T^* and q^* from which estimates of the surface fluxes can be calculated.

IMPACT AND APPLICATIONS

Economic Development

Landfalling hurricanes are one of the most costly natural disasters in the US and worldwide. The wave model and fully coupled modeling system developed from this NOPP project will be used in a coastal planning program in South Florida for estimation of hurricane impacts on the local community.

Quality of Life

Improved hurricane intensity forecasts can potentially save lives through a more effective warning and response system. We have been working with social scientists at the University of Miami to conduct idealized online and field survey using the coupled model hurricane simulations to study human behavior and decision making process.

Science Education and Communication

Hurricane forecast products from the NOPP supported high-resolution coupled model, such as the detailed rainfall, winds, waves, and currents have been incorporated in a new course at the University of Miami: *MSC 106: Hurricane and Society*. It is an interdisciplinary course on the meteorology of hurricanes, forecasting methods, and the societal and economic impact of the storms.

RELATED PROJECTS

The PIs from RSMAS/UM (Shuyi Chen and M. Donelan) and NRL-MRY (Sue Chen, H. Jin, S. Wang, and J. Doyle) are on the science team for the Impact of Typhoons on Ocean over the Pacific (ITOP) that collected unprecedented air-sea data including airborne dropsondes, AXBTs/ACDTs, EX-APEX floats, surface drafters and sea gliders, over the West Pacific during the ITOP field campaign from August-October 2010. These data will be used to evaluate and validate coupled model results.

Observations used for coupled model evaluation and verification are from projects led by Dr. Elizabeth Sanabia (AXBTs) and Dr. Tamay Ozgokomem and Dr. Luca Centinioni (drifters).

Shuyi Chen is a Co-PI on a NSF supported research project Understanding Dynamic Responses to Hurricane Warnings - Implications for Communication and Research. It uses the coupled model forecasts from the NOPP project to better understand how the forecast information is communicated and used in decision making process.

REFERENCES

- Bao, J.-W., C.W. Fairall, S. A. Michelson, L. Bianco, 2011: Parameterizations of sea-spray impact on the air-sea momentum and heat fluxes, *Mon. Wea. Rev.*, **139**, pp. 3781-3797.
- Chen, S. S., J. F. Price, W. Zhao, M. A. Donelan, and E. J. Walsh, 2007: The CBLAST-Hurricane Program and the next-generation fully coupled atmosphere-wave-ocean models for hurricane research and prediction. *Bull. Amer. Meteor. Soc.*, **88**, 311-317.

- Donelan, M. A., 1999: Wind-induced growth and attenuation of laboratory waves. Proceedings edited by S. G. Sajjadi, N. H. Thomas and J. C. R. Hunt, Wind-over-Wave Couplings, Clarendon Press, 183-194.
- Donelan, M. A., 2001: A nonlinear dissipation function due to wave breaking. Proceedings of the ECMWF workshop on Ocean Wave Forecasting, edited by P.A.E.M. Janssen, *European Centre for Medium-Range Weather Forecasts*, Reading, 87-94.
- Fairall, C. W., M. L. Banner, W. L. Peirson, W. Asher, and R. P. Morison, 2009: Investigation of the physical scaling of sea spray spume droplet production. *J. Geophys. Res.*, **114**, C10001, doi:10.1029/2008JC004918.
- Hasselmann, K., T. P. Barnett, E. Bouws, H. Carlson, D. E. Cartwright, K. Enke, J. A. Ewing, H. Gienapp, D. E. Hasselmann, P. Kruseman, A. Meerburg, P. Miller, D. J. Olbers, K. Richter, W. Sell, H. Walden, 1973: Measurements of wind-wave growth and swell decay during the Joint North Sea Wave Project (JONSWAP). *Ergänzungsheft zur Deutschen Hydrographischen Zeitschrift Reihe* **12**.
- Moon I-J, I. Ginis, and T. Hara, 2004: Effect of surface waves on Charnock coefficient under tropical cyclones: *Geophys. Res. Letters*, vol 31, L20302, doi:10.1029/2004GL020988.
- Kantha L. H. and C. A. Clayson, 2004: On the effect of surface gravity waves on mixing in an oceanic mixed layer. *Ocean Modell.*, **6**, 101–124.
- Kundu, P.K., (1976). Ekman veering observed near the ocean bottom, *J. Phys. Oceanogr.*, **6**: 238-242.
- Kuzmic, M., I. Janekovic, J. W. Book, P. J. Martin, and J. D. Doyle, (2006). Modeling the northern Adriatic double-gyre response to intense bora wind: A revisit, *J. Geophys. Res.*, **111**: C03S13.
- Hwang, P. A. (2011): A note on the ocean surface roughness spectra. Submitted to *J. Geophysical Research*.
- Rogers, W. E., A. V. Babanin, and D. W. Wang (2011). Observation-based input and whitecapping-dissipation in a model for wind-generated surface waves: Description and simple calculations. Accepted for publication in *J. Ocean Tech.*
- Teague, W. J., E. Jarosz, D. W. Wang, D. A. Mitchell, (2007): Observed Oceanic Response over the Upper Continental Slope and Outer Shelf during Hurricane Ivan. *J. Phys. Oceanogr.*, **37**: 2181–2206.
- Van Roekel, L. P., B. Fox-Kemper, P. P. Sullivan, P. E. Hamlington, and S. R. Haney (2012), The form and orientation of Langmuir cells for misaligned winds and waves, *J. Geophys. Res.*, **117**, C05001, doi:10.1029/2011JC007516.

PUBLICATIONS

- Baranowski, D., P.J. Flatau, S. Chen, P.G. Black, 2012: Air-sea interaction in two co-located typhoons. *Submitted to JPO, in revision*.
- Chen, S., T. J. Campbell, H. Jin, S. Gaberšek, R. M. Hodur, and P. Martin, 2010: Effect of two-way air-sea coupling in high and low wind speed regimes, *MWR*, **138**, 3579–3602.
- Chen, S. S., W. Zhao, M. A. Donelan, and H. L. Tolman, 2012a: Directional wind-wave coupling in fully coupled atmosphere-wave-ocean models: Results from CBLAST-Hurricane, *J. Atmos. Sci.*, in revision.
- Chen, S. S., W. Zhao, C.-Y. Lee, J. F. Price, and T. Sanford, 2012b: Fully coupled model simulations of three Atlantic hurricanes: Air-sea fluxes and pressure-wind relationship, *J. Atmos. Sci.*, submitted.

- Donelan, M. A., M. Curcic, S. S. Chen, and A. K. Magnusson, 2012: Modeling waves and wind stress, *J. Geophys. Res.*, **117**, doi:10.1029/2011JC007787.
- Judt, F., and S. S. Chen, 2010: Convectively Generated Potential Vorticity in Rainbands and Formation of Secondary Eyewall in Hurricane Rita of 2005, *J. Atmos. Sci.*, **67**, 3581–3599.
- Lee, C.-Y., and S. S. Chen, 2012: Symmetric and asymmetric structures of hurricane boundary layer in coupled atmosphere-wave-ocean models and observations, *J. Atmos. Sci.*, **69**, in press.
- Sanabia, E.R., B. Barrett, P.G. Black, S. Chen, J.A. Cummings, 2012: Implementation of upper-ocean temperature measurements in operational hurricane reconnaissance: successes and challenges from the 2011 AXBT Demonstration Project. *Submitted to Weather and Forecasting*.
- Smith, T.A., S. Chen, T. Campbell, E. Rogers, S. Gabersek, D. Wang, S. Carroll, R. Allard, 2012: A study of air-sea-wave interaction in COAMPS-TC: Hurricane Ivan (2004). *Submitted to Ocean Dynamics, in revision*.

CONFERENCE/JOURNAL SUBMISSIONS:

- Allard, R., T. A. Smith, E. Rogers, T. G. Jensen, P. Chu, T. Campbell, U. Gravois, S. Carroll, K. Watson: Validation Test Report for the Coupled Ocean Atmosphere Mesoscale Prediction System (COAMPS) Version 5.0: Ocean/Wave Component Validation, NRL Memorandum Report # 9423.
- Chen S., P. Harr, R. Elsberry, M. Peng, P. Black, J. Schmidt, R. Mrvaljevic, E D'Asaro, R.-C. Lien, T. Sanford, L. Centurioni, J. Morzel, H. Grabeg, 2012: Validation of Air-Ocean-Wave Coupled Simulation of Typhoon Fanapi, 2012 Fall AGU meeting, 3-7 December, San Francisco, CA.
- Chen, S. J. Cummings, P.G. Black, E. Sanabia, 2012:Forecasting rapid intensity changes with land-falling tropical cyclones, 10th symposium on the coastal environment, 22-26 Jan 2012, New Orleans, Louisiana.
- Smith, T. A., S. Chen, T. Campbell, E. Rogers, D. Wang, and R. Allard: Air-Sea-Wave Coupled Modeling of Western North Pacific Typhoon Fanapi (September 2010), AGU 2012 Ocean Sciences Meeting, Salt Lake City, UT, February 2012.
- Smith, T. A., S. Chen, T. Campbell, E. Rogers, S. Gabersek, D. Wang, and S. Carroll: Air-Ocean-Wave Coupling of Hurricane Ivan in COAMPS-TC (September 2004), AMS 30th Conf. on Hurricanes & Tropical Meteorology, Ponte Verde Beach, FL, April 2012.
- Jin, H., S. Wang, J. Doyle, S. Chen, 2012:Coupled COAMPS-TC real-time experiment for ITOP experiment. 30th conference on hurricane and tropical meteorology, 15-20 April 2012, Ponte Verde Beach, Florida.